Response of non-structural components mounted on irregular RC buildings: comparison between FE and EC8 predictions

Ayad B. Aldeka[*1], Andrew H.C. Chan[2a] and Samir Dirar[1b]

[1]*School of Civil Engineering, University of Birmingham, Edgbaston, Birmingham, B15 2TT, United Kingdom*
[2]*School of Science, Information Technology and Engineering, Federation University Australia, Victoria,*
Australia 3350 (formerly School of Civil Engineering, University of Birmingham)

Abstract.   This paper investigates the seismic response of lightweight acceleration-sensitive non-structural components (NSCs) mounted on irregular reinforced concrete (RC) primary structures (P-structures) using non-linear dynamic finite element (FE) analysis. The aim of this paper is to study the influence of NSC to P-structure vibration period ratio, peak ground acceleration, NSC to P-structure height ratio, and P-structure torsional behaviour on the seismic response of the NSCs. Representative constitutive models were used to simulate the behaviour of the RC P-structures. The NSCs were modelled as vertical cantilevers fixed at their bases with masses on the free ends and varying lengths so as to match the frequencies of the P-structures. Full dynamic interaction is considered between the NSCs and P-structures. A set of 21 natural and artificial earthquake records were used to evaluate the seismic response of the NSCs. The numerical results indicate that the behaviour of the NSCs is significantly influenced by the investigated parameters. Comparison between the FE results and Eurocode (EC8) predictions suggests that EC8 underestimates the response of NSCs mounted on the flexible sides of irregular RC P-structures when the fundamental periods and heights of the NSCs match those of the P-structures. The perceived cause of this discrepancy is that EC8 does not take into account the amplification in the dynamic response of NSCs induced by the torsional behaviour of RC P-structures.

Keywords: dynamic analysis; Eurocode 8; finite element; irregular RC buildings; non-structural components; torsion

1. Introduction

Multi-storey structures with complicated geometries have become widespread due to novel materials, advanced construction techniques, and modern architectural requirements. In such structures with plan irregularities, significant torsional effects induced by moderate and strong earthquakes are usually responsible for the damage to the structure and non-structural components (NSCs) (Chandler and Hutchinson 1986).

As it is important for safety and economic purposes to reduce the damage to NSCs during

∗Corresponding author, Ph.D. Candidate, E-mail: abb037@bham.ac.uk
[a]Professor, E-mail: a.chan@federation.edu.au
[b]Ph.D., Lecturer in Structural Engineering, E-mail: s.m.o.h.dirar@bham.ac.uk

earthquakes, extensive research efforts have concentrated on evaluating the seismic response of NSCs as well as their dynamic interaction with primary structures (P-structures). State of the art reviews (Chen and Soong 1988, Phan and Taylor 1996, Villaverde 1997, Whittaker and Soong 2003) categorised previous research on NSCs into studies that considered: (i) NSCs mounted on regular (i.e. without significant torsional effects) elastic P-structures, (ii) NSCs mounted on regular inelastic P-structures, and (iii) NSCs mounted on P-structures with torsional effects. The number of studies on NSCs attached to regular P-structures has largely exceeded the number of studies on NSCs attached to P-structures with torsional effects.

Realizing that the torsional behaviour of a P-structure can have an explicit effect that may amplify the seismic response of NSCs, Yang and Huang (1993, 1998) proposed an analytical method to evaluate the seismic behaviour of light equipment attached to P-structures with and without base isolation. Their approach, which included Rayleigh damping, was restricted to elastic P-structures with eccentricities in one direction between their centres of mass (CM) and centres of rigidity (CR). Agrawal and Datta (1997, 1998) studied the response of a secondary element mounted over an inelastic one-storey primary system (P-system) with significant torsional effects and subjected to a ground motion in one direction. They developed a two-dimensional model with the eccentricity between the CM and CR of the P-system in one direction (Agrawal and Datta 1997). They also studied the dynamic response of a secondary element mounted on an irregular inelastic P-system subjected to random ground motions in two orthogonal directions. The ground motions were represented as a broadband stationary random process. Sets of coupled differential equations were used to evaluate the hysteretic force-deformation behaviour of the P-system whereas linear frequency domain spectral analysis was used to evaluate the behaviour of secondary elements (Agrawal and Datta 1998, Agrawal 1999).

Mohammed *et al.* (2008) investigated experimentally the effect of both stiffness eccentric and mass eccentric P-systems on the seismic response of NSCs. The modelled P-systems, which were subjected to a unidirectional base motion, comprised a square aluminium platform (300 mm × 300 mm) supported at its corners by 3 mm diameter aluminium rods with varied lengths for stiffness adjustment. The NSCs were modelled as a lumped mass and were either rigid or near tuned to the fundamental vibration periods of the P-systems. The results showed that the torsional yielding of the P-systems had significant implications on the de-amplification of the seismic response of near tuned NSCs. However, Mohammed *et al.* (2008) concluded that their results were valid only for the investigated systems and cannot be generalised.

In the above-mentioned studies, analytical solutions and limited experimental investigations focused on the seismic response of NSCs mounted over either irregular P-systems with eccentricities in one direction between their CM and CR or irregular single-bay P-structures with eccentricities in two directions. However, the structural layouts and composite materials used in present-day P-structures are too complicated for an analytical solution to be available and research studies addressing the seismic response of NSCs attached to such P-structures are scarce.

One possible solution to bridge the knowledge gap in this area is to use advanced numerical methods such as finite element (FE) analysis. This paper presents non-linear dynamic FE analyses of NSCs mounted on inelastic irregular reinforced concrete (RC) multi-storey structures with torsional effects. It extends the work carried out by the authors on the same topic (Aldeka *et al.* 2012, 2013a, 2013b). The NSCs considered in this paper are lightweight acceleration-sensitive mechanical, electrical or medical equipment such as those found in industrial, commercial or healthcare buildings respectively. Normally, only the fundamental modes of such NSCs are of importance therefore they can be modelled as vertical cantilevers fixed at their bases with lumped

masses on their free ends (Yang and Huang 1993, 1998, Agrawal and Datta 1997, 1998, Agrawal 1999, Mohammed *et al.* 2008, Chudhuri and Villaverde 2008, Opropeza *et al.* 2010).

The main objectives of this paper are:

1. To investigate the influence of NSC to P-structure vibration period ratio, peak ground acceleration (PGA), NSC to P-structure height ratio, and P-structure torsional behaviour on the seismic response of NSCs.
2. To quantify the amplification in the dynamic response of NSCs induced by the torsional behaviour of RC P-structures.
3. To compare the predictions of the non-linear dynamic FE analyses with those of Eurocode 8 (EC8 2004) seismic design provisions for NSCs.

In the following sections, the rationale adopted for the selection of the RC P-structures considered in this study is explained. The characteristics and modelling of the P-structures and NSCs considered in this study are then detailed. The earthquake records used in the dynamic analyses are presented. Subsequently, the FE code used in this study is validated. Average numerical results of 2208 nonlinear dynamic FE analyses of the primary-secondary (P-S) systems are presented. The numerical response of the NSCs is compared with EC8 (2004) predictions. Finally, based on the obtained results, conclusions are drawn.

2. RC P-structures: selection, characteristics, and modelling

In order to validate the FE code used in this study and establish the credibility of the FE results, it was deemed necessary to base the numerical investigation on physically tested and/or previously modelled RC P-structures with significant torsional behaviour. The irregular three-storey RC P-structures "SPEAR (henceforward referred to as "Test")" (Negro *et al.* (2004), "Test 0.15", "Test 0.25" and "EC8 M" (Rozman and Fajfar 2009)) were therefore selected as P-structures in this study and their plan layout is used as the basic plan layout for this study. Additional five variants of "EC8 M"; i.e. "EC8 M5", "EC8 M7", "EC8 M10", "EC8 M13", and "EC8 M15"; were designed according to EC8 (2004) so as to provide a range of parameters (i.e. vibration periods, total heights, and torsional response) that may be used to study the dynamic behaviour of NSCs attached to RC P-structures with significant torsional behaviour.

The set of nine irregular RC P-structures can be divided into two groups. The first group includes four irregular RC P-structures (Test, Test 0.15, Test 0.25 and EC8 M) with similar total height (9 m) but different design characteristics as detailed in Section 2.1. The second group includes five irregular RC P-structures (EC8 M5, EC8 M7, EC8 M10, EC8 M13, and EC8 M15) with similar design characteristics but different total heights (15 m, 21 m, 30 m, 39 m, and 45 m) as detailed in Section 2.2. This strategy represented the most straightforward approach to consider RC P-structures with different vibration periods, heights, and torsional behaviour. In order to keep the number of analyses manageable, significant change to the plan layout has not been considered but this could be considered in future work.

2.1 First group of buildings

The first group of buildings includes the four irregular three-storey RC P-structures Test, Test 0.15, Test 0.25, and EC8 M which have the same plan layout and total height (9 m) but different cross-sectional dimensions and steel reinforcement details. Fig. 1(a) shows that these buildings

have eccentricities in two directions between their CM and CR. The typical floor height is 3 m as shown in Fig. 1(b). The buildings have significant torsional behaviour as demonstrated by the third modal shape shown in Fig. 1(c). Table 1 details the characteristics of the first group of buildings.

(a)   (b)   (c)
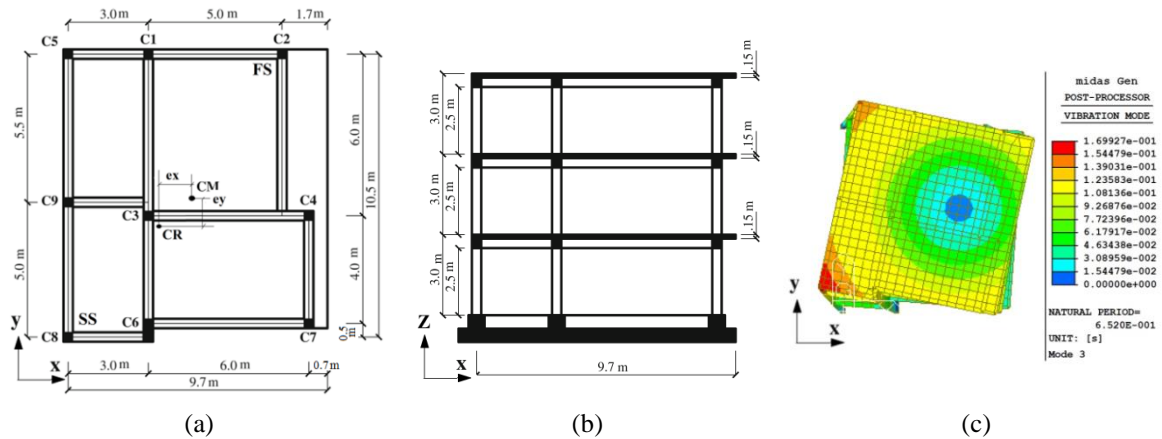
Fig. 1 First group of buildings: (a) plan, (b) elevation (Rozman and Fajfar 2009) and (c) torsional mode

Table 1 Description and design characteristics of the first group of buildings

Building	Description and design characteristics	Eccentricity [m]	
		e_x	e_y
Test	SPEAR Structure (Negro *et al.* 2004) – designed to resist vertical loads only (permanent load of 0.5 kN/m² was used). Total height = 9 m.	1.30	1.00
Test 0.15	Had the same vertical load, plan layout, total height, and cross-sectional dimensions as Test. Designed using the EC8 (2004) type 1 spectrum for ground type C (a_g = 0.15 g, behaviour factor (q) = 3.45, soil factor (S) = 1.15, design acceleration on type C ground = 0.17 g)	1.30	1.00
Test 0.25	Had the same vertical load, plan layout, total height, and cross-sectional dimensions as Test. Designed using the EC8 (2004) type 1 spectrum for ground type C (a_g = 0.25 g, q = 3.45, S = 1.15, design acceleration on type C ground = 0.29 g)	1.30	1.00
EC8 M	Had the same plan layout and total height as Test. Permanent load of 2.7 kN/m² was used. The cross-sectional dimensions of the beams and columns were increased in order to meet the EC8 (2004) Ductility Class M requirements. Designed using the EC8 (2004) type 1 spectrum for ground type C (a_g = 0.25 g, q = 3.45, S = 1.15, design acceleration on type C ground = 0.29 g)	0.99	0.73

Building Test (Negro *et al.* 2004) was designed to resist vertical loads only. The characteristic permanent floor load was taken as 0.5 kN/m². Its cross-section details are given in Table 2.

Buildings Test 0.15 and Test 0.25 had the same vertical load, plan layout, total height, and cross-sectional dimensions as Test. They were designed using the EC8 (2004) type 1 spectrum for ground type C. Test 0.15 was designed for a design ground acceleration on type A ground (a_g) of 0.15 g whereas Test 0.25 was designed for an a_g of 0.25 g. Considering the soil factor of 1.15 for

Table 2 Cross-section details of the first group of buildings (all dimensions in mm)

Building	Beams			Columns					
				C1,C2,C3,C4,C5,C7,C8,C9			C6		
	Cross section	Long. steel	Shear steel	Cross section	Long. steel	Shear steel	Cross section	Long. steel	Shear steel
Test	250×500	6Ø 12	Ø 8@200	250×250	4Ø 12	Ø 8@250	250×750	10Ø 12	Ø 8@250
Test 0.15	250×500	6Ø 14	Ø 8@100	250×250	8Ø 16	Ø 6@100	250×750	16Ø 16	Ø 6@80
Test 0.25	250×500	6Ø 14	Ø 8@100	250×250	6Ø 20	Ø 6@100	250×750	14Ø 22	Ø 6@80
EC8 M	350×450	9Ø 16	Ø 8@90	350×350	Table 3	Ø 8@120	350×850	Table 3	Ø 8@120

Table 3 Longitudinal steel reinforcement in the columns of EC8 M

Storey	C1	C2	C3	C4	C5	C6	C7	C8	C9
1st & 2nd	8Ø 25	8Ø 22	4Ø 22+ 4Ø 25	8Ø 22	8Ø 22	16Ø 22	8Ø 20	8Ø 22	8Ø 20
3rd	8Ø 20	8Ø 20	8Ø 20	8Ø 20	8Ø 16	16Ø 22	4Ø 16+ 4Ø 20	8Ø 16	8Ø 16

ground type C, the design ground accelerations on type C ground for Test 0.15 and Test 0.25 were 0.17 g and 0.29 g respectively. The steel reinforcement amounts used in Test 0.15 and Test 0.25 were higher than those amounts used in Test (see Table 2). However, the beam and column cross-sectional dimensions of Test 0.15 and Test 0.25 did not fully meet the EC8 (2004) requirements. The values of the over-strength factor (γ_{Rd}) for Test 0.15 and Test 0.25 were 0.40 and 0.65 respectively. Hence Test 0.15 and Test 0.25 did not fulfil the EC8 (2004) global and local ductility requirements (Rozman and Fajfar 2009). Nonetheless, Test 0.15 and Test 0.25 were considered in this study for two reasons. Firstly, they are representative of building practice before the adoption of modern seismic codes (Rozman and Fajfar 2009). Secondly, as their seismic capacities were higher than the basic model, i.e. Test, they availed the opportunity to study the effect of P-structure seismic capacity on the seismic response of NSCs. However, it should be noted that it might be incorrect to compare the response of NSCs attached to Test 0.15 and Test 0.25 with EC8 (2004) predictions. In this paper, only the response of the NSCs attached to the P-structures that fully met the EC8 (2004) requirements are used to evaluate the accuracy of EC8 (2004) seismic design guidelines for NSCs.

EC8 M had the same plan layout and total height as Test. It was designed using the EC8 (2004) type 1 spectrum for ground type C. EC8 M was designed for an a_g value of 0.25 g. Considering the soil factor of 1.15 for ground type C, the design ground acceleration on type C ground for EC8 M was 0.29 g. The characteristic permanent floor load was taken as 2.7 kN/m^2 instead of 0.5 kN/m^2. The cross-sectional dimensions and amounts of steel reinforcement were increased in the case of EC8 M - compared to Test, Test 0.15, and Test 0.25 (see Tables 2 and 3) - in order to meet the EC8 (2004) Ductility Class M requirements. EC8 M had a γ_{Rd} value of 1.30 and fulfilled all EC8 (2004) global and local ductility requirements (Rozman and Fajfar 2009).

Concrete Class C25/30 and steel reinforcement Grade 400 were used in all buildings except Test which had steel yield strength of 459 MPa (Rozman and Fajfar 2009). Further information can be found in Negro *et al.* (2004) for Building Test and in Rozman and Fajfar (2009) for Buildings Test 0.15, Test 0.25 and EC8 M.

2.2 Second group of buildings

The second group of buildings consists of the five irregular RC P-structures EC8 M5, EC8 M7, EC8 M10, EC8 M13, and EC8 M15 which have the same plan layout and storey height as the first group of buildings but differ in the total height, beam and column cross-sectional dimensions, and steel reinforcement details. In order to represent low- and medium-rise RC P-structures, building heights in the range of 15-45 m were considered as detailed in Table 4.

The second group of buildings satisfied the EC8 (2004) Ductility Class M requirements. They were designed by the authors using the EC8 (2004) type 1 spectrum for ground type C and an a_g value of 0.25 g. Considering the soil factor of 1.15 for ground type C, their design ground acceleration on type C ground was 0.29 g. Based on EC8 (2004) provisions, the value of 3.45 was selected for the behaviour factor (q). Concrete Class C25/30 and steel reinforcement Class C S500 were used in the design of the second group of buildings. The characteristic values of the floor loads were taken as 2.7 kN/m^2 and 2.0 kN/m^2 for permanent and variable actions respectively.

Table 4 Cross-section details of the second group of buildings (all dimensions in mm)

Building	Storey	Columns				Shear hoops (critical region)	Joint shear hoops	Beams		
		C1,C2,C3,C4, C5,C7,C8,C9		C6				Cross-section	Long. Steel: bottom[*] top[+]	Shear steel
		Cross-section	Long. steel	Cross-section	Long. steel					
EC8 M5 (15 m high)	1-2	450×450	16Ø 20	450×1000	20Ø 20	2Ø 8 @120	3Ø 8 @100	350×500	5Ø 16[*] 4Ø 16[+]	Ø 8 @90
	3-5	400×400	16Ø 20	400×850	20Ø 20					
EC8 M7 (21 m high)	1-2	550×550	24Ø 20	550×1150	30Ø 20	2Ø 8 @110	3Ø 8 @90	350×500	6Ø 16[*] 4Ø 16[+]	Ø 8 @90
	3-4	500×500	24Ø 20	500×1000	28Ø 20					
	5-7	450×450	16Ø 20	450×850	20Ø 20					
EC8 M10 (30 m high)	1-2	650×650	30Ø 20	650×1200	34Ø 20	3Ø 8 @110	3Ø 8 @90	350×500	8Ø 16[*] 5Ø 16[+]	Ø 8 @90
	3-4	600×600	30Ø 20	600×1100	30Ø 20					
	5-7	550×550	24Ø 20	550×950	28Ø 20	2Ø 8 @110				
	8-10	500×500	16Ø 20	500×800	22Ø 20					
EC8 M13 (39 m high)	1-2	750×750	24Ø 25	800×1200	26Ø 25	3Ø 8 @90	3Ø 8 @90	400×600	10Ø 16[*] 7Ø 16[+]	Ø 8 @100
	3-4	650×650	24Ø 25	700×1000	24Ø 25					
	5-7	650×650	24Ø 25	700×1000	24Ø 25					
	8-10	600×600	20Ø 25	650×950	22Ø 25					
	11-13	500×500	16Ø 25	500×850	16Ø 25	2Ø 8 @90				
EC8 M15 (45 m high)	1-2	850×850	30Ø 25	850×1250	32Ø 25	3Ø 8 @90	3Ø 8 @90	450×650	7Ø 20[*] 6Ø 20[+]	Ø 8 @100
	3-4	750×750	30Ø 25	750×1000	32Ø 25					
	5-6	700×700	28Ø 25	700×900	28Ø 25					
	7-9	650×650	24Ø 25	650×800	24Ø 25					
	10-12	600×600	20Ø 25	600×700	18Ø 25					
	13-15	500×500	16Ø 25	500×550	16Ø 25	2Ø 8 @90				

2.3 Modelling of the RC P-structures

The cross-sections of the RC P-structures were modelled with distributed inelastic fiber elements as shown in Fig. 2. This modelling approach leads to an accurate representation of the geometrical and mechanical properties of each member.
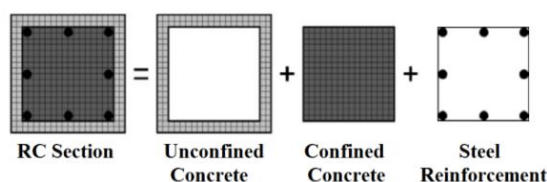

Fig. 2 Description of a reinforced concrete section as implemented in MIDAS Gen code (2012)

The confined and unconfined concrete models proposed by Mander *et al.* (1988) and the steel reinforcement model by Menegotto and Pinto (1973), which are available in MIDAS Gen code (2012), were used. The input parameters required to define the concrete models are the cylinder compressive strength (taken as 25 MPa) and the unconfined concrete peak strain (taken as 0.002). The concrete elastic modulus, tensile strength, and tensile strain are automatically computed by the FE code (MIDAS Gen 2012). The input parameters required to describe the steel model proposed by Menegotto and Pinto (1973) are the yield strength (taken as reported in Sections 2.1 and 2.2), initial elastic modulus (taken as 206 GPa), strain hardening ratio (taken as 0.005 for ordinary steel bars), and three constants (R_o, a_1, a_2) required to control the transition from the elastic to the plastic branch of the steel constitutive model. The recommended values of these constants for ordinary steel bars are 20 for R_o, 18.5 for a_1, and 0.15 for a_2 (Menegotto and Pinto 1973). Newmark's method was used to integrate the equations of motion of the system, performing full Newton-Raphson iterations until convergence was achieved. The constant acceleration method was adopted with Newmark's time integration parameters, γ and β, taken as 0.5 and 0.25 respectively. A damping ratio of 5%, based on the recommendations of Paz (1994), was used for the P-structures.

The experimental investigation by Negro *et al.* (2004), on which parts of this study are based, employed the elastic spectra of the longitudinal and transverse components of Herceg-Novi records (extracted from the European Strong-motion Database (ESD)) which are consistent with the EC8 (2004) type 1 spectrum for ground type C. Hence, for comparison purposes, all buildings were assumed to be constructed on ground type C (deep deposits of dense or medium-dense sand, gravel or stiff clay). However, further research work carried out by the authors (not reported here due to paper length limitations) has shown that the conclusions drawn are not limited to this ground type.

2.4 Eigenvalue analysis of the RC P-structures

Eigenvalue analyses were performed to calculate the vibration periods of the studied buildings. The vibration periods of the first nine modes (transitional modes in X and Y directions and torsional modes (see Fig. 1)) are presented in Table 5.

Table 5 Vibration periods of the studied buildings

Building	Vibration periods [s]								
	T_1	T_2	T_3	T_4	T_5	T_6	T_7	T_8	T_9
Test, Test 0.15, Test 0.25	0.823	0.735	0.655	0.339	0.301	0.246	0.223	0.213	0.162
EC8 M	0.550	0.522	0.421	0.171	0.152	0.130	0.126	0.115	0.112
EC8 M5	0.660	0.640	0.510	0.210	0.200	0.160	0.120	0.110	0.100
EC8 M7	0.840	0.830	0.660	0.270	0.260	0.210	0.150	0.140	0.110
EC8 M10	1.170	1.150	0.920	0.380	0.370	0.280	0.210	0.200	0.160
EC8 M13	1.290	1.260	1.020	0.430	0.420	0.310	0.240	0.230	0.180
EC8 M15	1.390	1.310	1.120	0.440	0.430	0.320	0.250	0.240	0.190

3. Non-structural components: selection, modelling, and characteristics

As explained in Section 1, the NSCs considered in this paper are lightweight acceleration-sensitive mechanical, electrical or medical equipment - such as those found in industrial, commercial or healthcare buildings - and normally only the fundamental mode is of importance therefore they can be modelled as cantilevers fixed at their bases.

Single-degree-of-freedom (SDOF) mechanical oscillators are commonly used to model such NSCs (Yang and Huang 1993, 1998, Agrawal and Datta 1997, 1998, Agrawal 1999, Mohammed *et al.* 2008, Chudhuri and Villaverde 2008, Opropeza *et al.* 2010). A modelling approach similar to that used by Sackman and Kelly (1979) was adopted in this study where the NSCs were modelled as vertical cantilevers fixed at their bases with masses on the free ends. Each cantilever had a $152 \times 152 \times 51$ mm³ lumped steel mass weighing about 9.25 kg. The arms of the cantilevers were modelled as circular sections, 40 mm in diameter. The circular cross-section was favoured because it has the same lateral stiffness in any horizontal direction. The length (L_a) and lateral stiffness (K_a) values of the circular cantilever arms are given in Table 6. These values were chosen in such a way that the NSC vibration periods (T_C) match one of the first three vibration periods (T_1, T_2, and T_3) of the P-structures. It should be noted that the first (T_1) and second (T_2) vibration periods of the second group of buildings were approximately equal (See Table 5). Hence, for the second group of

Table 6 Characteristics of the NSCs considered in this study

Building	NSCs with $T_C = T_1$			NSCs with $T_C = T_2$			NSCs with $T_C = T_3$		
	L_a [m]	K_a [N/m]	T_C [s]	L_a [m]	K_a [N/m]	T_C [s]	L_a [m]	K_a [N/m]	T_C [s]
Test, Test 0.15, Test 0.25	2.29	533.6	0.82	2.12	672.5	0.73	1.96	851.0	0.65
EC8 M	1.75	1195.6	0.55	1.69	1327.5	0.52	1.46	2059.9	0.42
EC8 M5	1.24	840.2	0.66	-	-	-	1.05	1383.8	0.51
EC8 M7	1.46	514.7	0.84	-	-	-	1.96	851.0	0.65
EC8 M10	1.82	265.7	1.17	-	-	-	1.55	430.2	0.92
EC8 M13	1.94	219.4	1.29	-	-	-	1.66	352.55	1.02
EC8 M15	2.04	188.7	1.39	-	-	-	1.77	288.9	1.12

buildings, only NSCs with vibration periods matching the first and third vibration periods of the P-structures were considered. Additional NSCs vibration periods were considered, as presented in Figs. 6 and 7, in order to investigate the influence of NSC to *P*-structure vibration period ratio.

Full dynamic interaction is considered between the NSCs and *P*-structures. A damping ratio of 3%, based on Graves and Morante (2006), was used for the NSCs.

4. Earthquake records

EC8 (2004) (Clause 4.3.3.4.3) allows the use of the mean effects of at least seven artificial, natural, or simulated earthquake records for design purposes. In order to increase confidence in the results of this study, a set of 21 earthquake records were used. This set consisted of seven pairs of natural records and seven artificial earthquakes, all of which are compatible with the EC8 (2004) type 1 response spectrum for ground type C.

Table 7 summarises the main characteristics of the seven pairs of natural records. The natural earthquakes were extracted from the ESD using the computer code REXEL Ver. 3.2 (beta) (Iervolino *et al.* 2009, 2010). This freely available software automatically selects earthquake records compatible with the EC8 (2004) elastic response spectra. The selected natural records were modified in such a way their pseudo accelerations were completely compatible with the EC8 (2004) type 1 spectrum for ground type C. The modification process of the natural records was implemented using the computer software SeismoMatch ver. 2.1 (Seismosoft 2009) which utilizes a procedure that modifies earthquake accelerograms to match a specific target response spectrum without increasing the number of motion cycles. As shown in Fig. 3, the mean pseudo accelerations of the selected natural ground motions in the X and Y directions match the pseudo accelerations of the EC8 (2004) type 1 spectrum for ground type C.

The seven artificial records were generated using SIMQKE (1976). This software generates a spectral density function from response spectrum data input and then obtains sinusoidal signals with random phase angles. The advantage of this approach is that it can obtain accelerograms completely compatible with the EC8 (2004) elastic response spectra but the disadvantage is that it generates an excessive number of strong motion cycles which have higher energy content. The EC8 (2004) type 1 elastic response spectrum for ground type C and a PGA value of 0.25 g were used as inputs to generate seven accelerograms with duration of 30 s each. Fig. 4 shows that the response spectrum of the mean of the seven artificial records matches quite well with the EC8

Table 7 Characteristics of the natural ground motion records

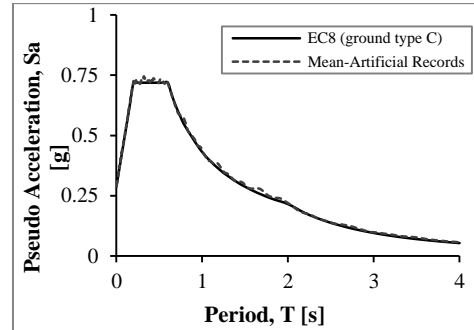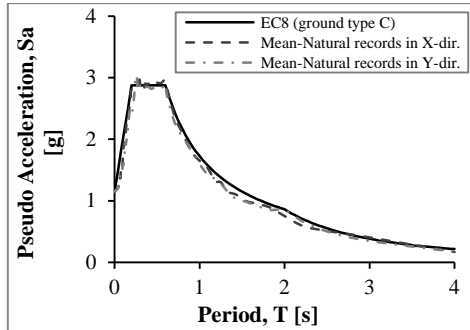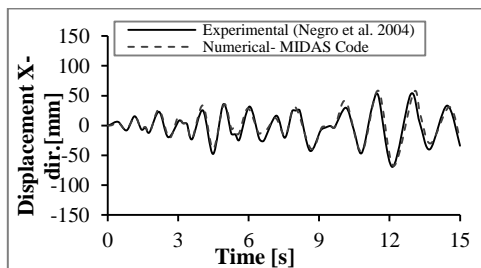| Code	Earthquake Name and Location	Station ID	Date	Mw	PGA-X [g]	PGA-Y [g]
000133	Friuli (aftershock)- Italy	ST33	15/09/1976	6	1.0686	0.9324
000333	Alkion- Greece	ST121	24/02/1981	6.6	2.2566	3.0363
000334	Alkion- Greece	ST122	24/02/1981	6.6	2.8382	1.6705
000335	Alkion- Greece	ST121	25/02/1981	6.3	1.1437	1.176
000600	Umbria Marche- Italy	ST223	26/09/1997	6	1.6852	1.0406
000879	Dinar- Turkey	ST271	01/10/1995	6.4	2.6739	3.1306
001726	Adana- Turkey	ST549	27/06/1998	6.3	2.1575	2.6442

Fig. 3 Response spectra of natural ground motions   Fig. 4 Response spectrum of artificial ground motions

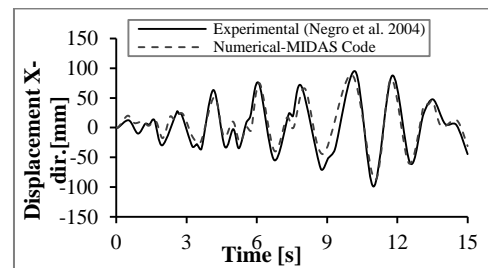(2004) type 1 spectrum for ground type C.

The natural and artificial records were used to investigate the behaviour of the NSCs mounted on the first and second groups of buildings respectively.
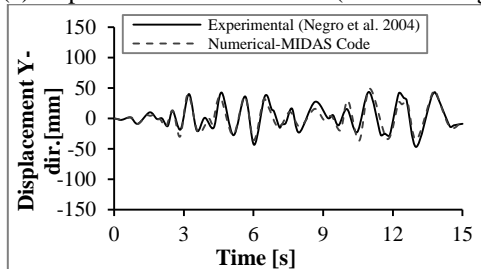
5. Validation of the FE code

This section summarises the validation of the FE code, MIDAS Gen Ver. 3.1 (2012), used in this study. The building selected for the validation of the software is Test (Negro *et al.* 2004) because of its significant torsional behaviour. During testing, the building was subjected to the Herceg-Novi record which was scaled to the PGA values of 0.15 g and 0.20 g. Only minor cracks concentrated at the top of columns and in the beams connected to Column C6 (see Fig. 1(a))

(a) displacement in *x*-direction (PGA = 0.15 g)   (b) displacement in *x*-direction (PGA = 0.20 g)

(c) displacement in *y*-direction (PGA = 0.15 g)   (d) displacement in *y*-direction (PGA = 0.20 g)

Fig. 5 Comparison between the experimental and numerical results for building test

(e) rotation *z* (PGA = 0.15 g)
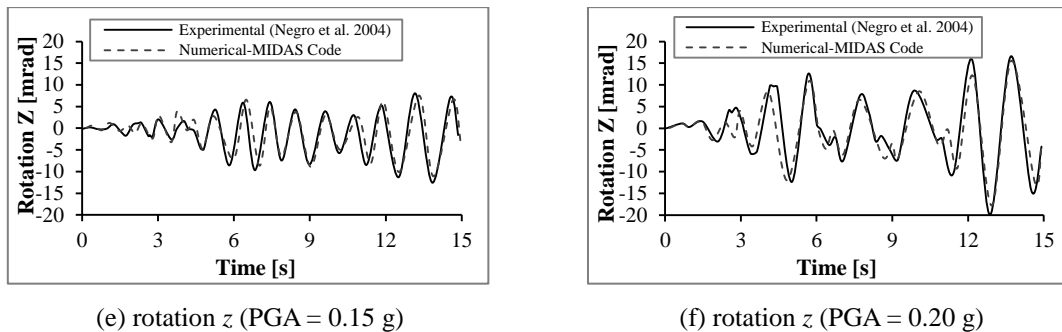
(f) rotation *z* (PGA = 0.20 g)

Fig. 5 Continued

occurred when the building was subjected to the 0.15 g PGA. When the building was subjected to the 0.20 PGA, the columns, especially those at the second floor, experienced higher damage levels. Some damage was also detected in the beams and floor slabs (Negro *et al.* 2004).

The FE model for Test was also subjected to the Herceg-Novi record scaled to the PGA values of 0.15 g and 0.20 g. The comparison between the numerical and experimental results included the top floor displacements in the X and Y directions and the rotations at the CM of the top floor (see Fig. 1(a)). As a result of the accurate modelling of the building, good agreement between the numerical results and the corresponding experimental results was achieved as shown in Fig. 5 and the predicted behaviour was representative of the inelastic behaviour of the structure. Based on the good agreement between the numerical and experimental results for Test, further numerical analyses were carried out to identify the influence of NSC to P-structure vibration period ratio, peak ground acceleration, NSC to P-structure height ratio, and P-structure torsional behaviour on the seismic response of NSCs.

6. Nonlinear static (push-over) analyses of the P-structures

Push-over analyses were carried out to calculate the elastic and maximum seismic capacities of the RC P-structures. The displacement values at near collapse were corrected by considering the torsional effects using the extension of the N2 procedure. The extended N2 procedure is a simplified nonlinear method for the seismic analysis of plan-asymmetric structures. It can be used to calculate the seismic capacities and the idealised force-displacement response of such structures by combining the results obtained by push-over analysis of a 3D structural model with the results of a linear dynamic spectral analysis (Fajfar *et al.* 2005). Further details on the extended N2 procedure can be found in Kreslin and Fajfar (2010), and Stefano and Pintucchi (2010).

For each building, Table 8 details the characteristics of the idealised elastic-perfectly plastic force-displacement relationship determined according to Annex B of EC8 (2004). The idealised force-displacement curves were used to calculate the elastic and maximum seismic capacities of the buildings. The values of the elastic and maximum seismic capacities of the P-structures are used in Sections 7 and 8 to interpret the numerical results and compare them with EC8 (2004) predictions. The initial stiffness of the idealized system is determined in such a way that the areas under the actual and idealized force-displacement curves are equal. For each building, the characteristics detailed in Table 8 are the maximum seismic capacity, weight (*W*), effective mass

(m^*), transformation constant (Γ), base shear (F_y), near collapse displacement (d_m), actual deformation energy (E_m), yield displacement (d_y), effective period of the idealized equivalent SDOF system (T^*), elastic acceleration response (S_{ae}) at T^*, acceleration at the yield point (S_{ay}), and target displacement of the multiple-degree-of-freedom system (d_t). It can be seen from Table 8 that the maximum seismic capacity for each building is given by the PGA value that corresponds to a value of d_m/d_t approximately equal to 1.0.

Table 8 Maximum seismic capacities and characteristics of the idealized force-displacement relationship

Building	Maximum seismic capacity [g]	W [kN]	m^* [kg].10^3	Γ	F_y [kN]	d_m [m]	E_m [kN.m]	d_y [m]	T^* [s]	S_{ae} [g]	S_{ay} [g]	d_t [m]	d_m/d_t
Test	0.26	1935.0	135.0	1.26	211.0	0.119	21.4	0.0347	0.94	0.43	0.12	0.118	1.01
Test 0.15	0.46	1935.0	141.0	1.24	444.0	0.168	63.6	0.0494	0.79	0.87	0.25	0.166	1.01
Test 0.25	0.51	1935.0	141.0	1.24	583.0	0.187	88.1	0.0717	0.83	0.89	0.33	0.188	1.00
EC8 M	0.76	2850.0	192.0	1.28	905.0	0.215	175.5	0.0722	0.59	1.89	0.37	0.213	1.01
EC8 M5	0.74	4536.6	308.1	1.36	1317.4	0.315	365.6	0.075	0.83	1.33	0.32	0.312	1.01
EC8 M7	0.69	6659.0	428.4	1.4	1519.4	0.385	509.0	0.100	1.05	0.97	0.26	0.376	1.02
EC8 M10	0.63	9993.9	628.0	1.43	1773.6	0.481	724.5	0.145	1.42	0.66	0.20	0.475	1.01
EC8 M13	0.58	14699.3	875.3	1.44	2134.3	0.521	930.6	0.170	1.66	0.52	0.17	0.511	1.02
EC8 M15	0.58	18515.6	1083.3	1.45	2571.6	0.552	1188.1	0.180	1.73	0.51	0.17	0.545	1.01

According to Annex B of EC8 (2004), a building is considered within the elastic range if its ductility factor (μ) is within the range of 0 to 1.0. Hence, the elastic seismic capacity may be defined as the PGA value corresponding to $\mu = 1.0$. Table 9 gives the elastic seismic capacities of the P-structures considered in this study together with the values of the spectral accelerations. The PGA values corresponding to the elastic seismic capacities were used, together with other PGA values, to study the seismic behaviour of the NSCs as detailed in Section 7.

Table 9 Elastic seismic capacities of the RC P-structures

Building	Elastic seismic capacity [g]	S_{ae} [g]	S_{ay} [g]	μ
Test	0.070	0.124	0.12	1.03
Test 0.15	0.100	0.256	0.25	1.02
Test 0.25	0.120	0.335	0.33	1.02
EC8 M	0.135	0.375	0.37	1.01
EC8 M5	0.160	0.33	0.32	1.03
EC8 M7	0.160	0.26	0.26	1.00
EC8 M10	0.160	0.20	0.20	1.00
EC8 M13	0.170	0.18	0.17	1.06
EC8 M15	0.170	0.17	0.17	1.00

It should be noted that the values of the elastic and maximum seismic capacities as well as the values of the elastic acceleration response (S_{ae}) and acceleration at the yield point (S_{ay}) reported in Tables 8 and 9 above are spectral acceleration values at the 1st mode period of each building. They should not be confused with the maximum ground acceleration for a given ground motion.

7. Dynamic response of the NSCs

The results presented hereinafter are based on averages of the NSCs response to the earthquake records detailed in Section 4. Due to space limitations, only selected results that detail the effect of the investigated parameters on the dynamic response of the NSCs are presented.

Due to the 3D nature of the P-structures considered in this study, there are two different peak component acceleration (*PCA*) values in the horizontal X and Y directions, i.e. PCA_x and PCA_y respectively. The resultant peak component acceleration (PCA_{xy}) is calculated as the square root of the sum of the squares of PCA_x and PCA_y.

In the following sections, reference will be made to the elastic and maximum seismic capacities for a given P-structure as given in Tables 9 and 8 respectively.

7.1 Effect of NSC to P-structure vibration period ratio

The NSC to P-structure vibration period ratio is one of the main parameters that affect the response of the NSCs. The importance of this parameter stems from the fact that the NSCs resonate when their vibration periods match the vibration periods of the P-structures. Fig. 6 shows the relationship between peak component acceleration and NSC to P-structure vibration period ratio (T_C/T_1) for the NSCs mounted on the flexible sides (FS, i.e. the side that undergoes the largest displacement - see Fig. 1(a)) of the top floors of the first group of buildings. Fig. 6(a) shows the results at the elastic seismic capacity (0.07 g, 0.10 g, 0.12 g, and 0.135 g) whereas Fig. 6(b) shows the results at the maximum seismic capacity (0.26 g, 0.46 g, 0.51 g, and 0.76 g) for Test, Test 0.15, Test 0.25, and EC8 M respectively.

Fig. 6 exhibits three zones of dynamic response. In Zone 1, NSCs accelerations increase gradually with the increase in T_C/T_1 from 0 to 0.68. In Zone 2, a sharp increase in NSCs accelerations occurs between T_C/T_1 values of 0.765 and 1.0. This was to be expected since the

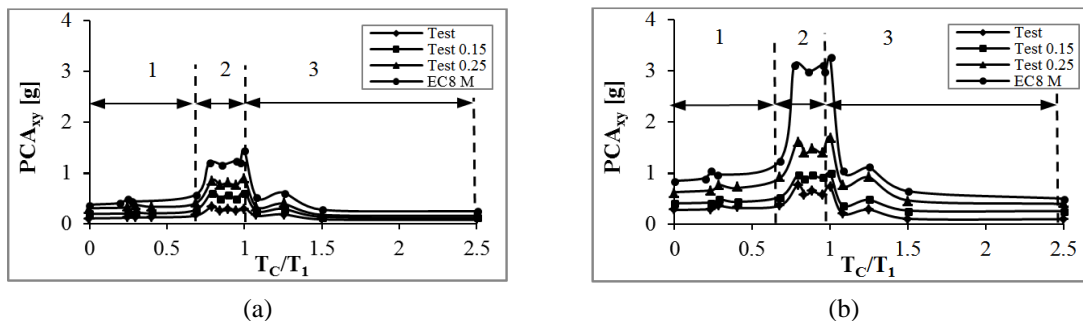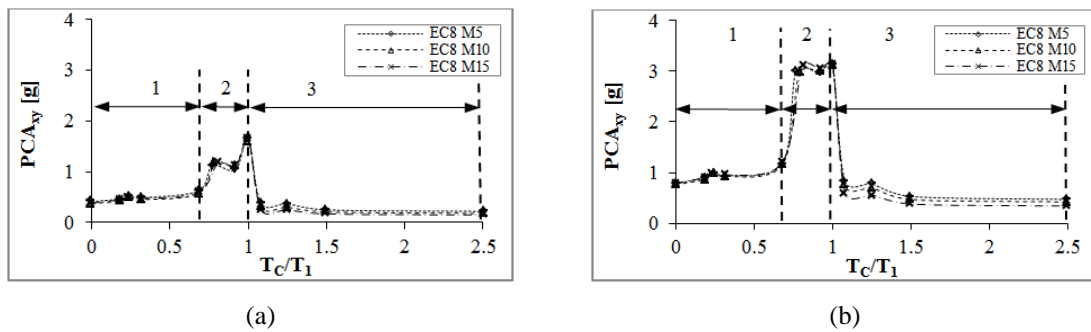(a)   (b)

Fig. 6 Variation of peak component acceleration vs. NSC to P-structure vibration period ratio for the NSCs mounted on the flexible sides of the top floors of the first group of buildings at: (a) the elastic seismic capacity and (b) the maximum seismic capacity for each building

NSCs resonate when their vibration periods match the third and first vibration periods of the P-structures at T_C/T_1 values of 0.765 and 1.0 respectively. Zone 3 is marked by a sudden drop in NSCs accelerations at T_C/T_1 values greater than 1.0.

For $T_C = T_1$, the NSCs accelerations at the maximum seismic capacities were on average 125% higher than the corresponding values at the elastic seismic capacities of the buildings. For a given T_C/T_1 value, the NSCs attached to EC8 M experienced the highest acceleration. This may be explained by the fact that this building had the highest elastic (0.135 g) and maximum (0.76 g) seismic capacities and hence was subjected to higher PGA values. On the other hand, the NSCs attached to Test experienced the lowest accelerations as this building had the least elastic (0.07 g) and maximum (0.26 g) seismic capacities.

Fig. 7 shows the variation of NSCs accelerations with T_C/T_1 for the NSCs attached to the flexible sides of the top floors of EC8 M5, EC8 M10, and EC8 M15. It can be seen from Fig. 7 that the NSCs attached to buildings from the second group had the same three-zone dynamic response experienced by the NSCs attached to the first group of buildings. For $T_C = T_1$, the NSCs accelerations at the maximum seismic capacities were on average 91% higher than the corresponding values at the elastic seismic capacities of the buildings.

Fig. 7 Variation of peak component acceleration vs. NSC to P-structure vibration period ratio for the NSCs mounted on the flexible sides of the top floors of EC8 M5, EC8 M10, and EC8 M15 at: (a) the elastic seismic capacity and (b) the maximum seismic capacity for each building

Unlike the NSCs mounted on the first group of buildings, the NSCs attached to EC8 M5, EC8 M10, and EC8 M15 had approximately the same response at a given T_C/T_1 value. The second group of buildings had approximately the same elastic seismic capacities (0.16 g – 0.17 g, see Table 9) hence there was no change in the NSCs response at this PGA value.

The maximum seismic capacities of EC8 M5, EC8 M10, and EC8 M15 were inversely proportional to their heights (see Table 8). This suggests that, for a given T_C/T_1 value, the NSCs attached to EC8 M15 and EC8 M10 should have lower acceleration values than the NSCs attached to EC8 M5. However, Fig. 7(b) shows clearly that the NSCs attached to EC8 M5, EC8 M10, and EC8 M15 had comparable response at the maximum seismic capacities of these P-structures. This result suggests that EC8 M15 and EC8 M10 had stronger torsional behaviour than EC8 M5. Consequently, the response of the NSCs attached to EC8 M15 and EC8 M10 was more amplified than the response of the NSCs attached to EC8 M5. Eventually, this resulted in the comparable response shown in Fig. 7(b). This result will be further investigated in Section 7.4.

7.2 Effect of peak ground acceleration

The effect of PGA on the seismic behaviour of the NSCs was investigated by considering PGA values in the range of 0.05 g to the maximum seismic capacity of each building. Fig. 8 displays the variation of peak component acceleration with PGA for the NSCs with $T_C = T_1$ and mounted on the flexible sides and centres of rigidity of the top floors of the P-structures considered in this study.

For a given P-structure in Fig. 8, NSCs accelerations vary approximately linearly with base excitation up to the PGA value corresponding to the elastic seismic capacity of the P-structure. At higher PGA values, damage reduces the global stiffness of the P-structure and consequently changes its dynamic characteristics. This, in turn, reduces the rate of increase of the P-structure and NSCs accelerations and results in a non-linear relationship between NSCs accelerations and PGA. Of note is that the NSCs attached to the flexible sides had accelerations that were on average 42% higher than the accelerations of the NSCs attached to the centres of rigidity.

Figs. 8(a) and 8(b) show that, for a given PGA value, the NSCs attached to EC8 M, which was designed according to EC8 (2004), had higher acceleration values than the corresponding NSCs attached to Test, Test 0.15, and Test 0.25; which were not in full compliance with EC8 (2004) provisions (see Section 2.1). Due to its relatively high stiffness, EC8 M had a lower fundamental vibration period (0.55 s) compared to the other three buildings which had a fundamental vibration period of 0.823 s. Hence, it experienced higher floor accelerations which, in turn, resulted in higher component accelerations. Conversely, the NSCs attached to Test, which was the least stiff building, experienced the lowest accelerations.
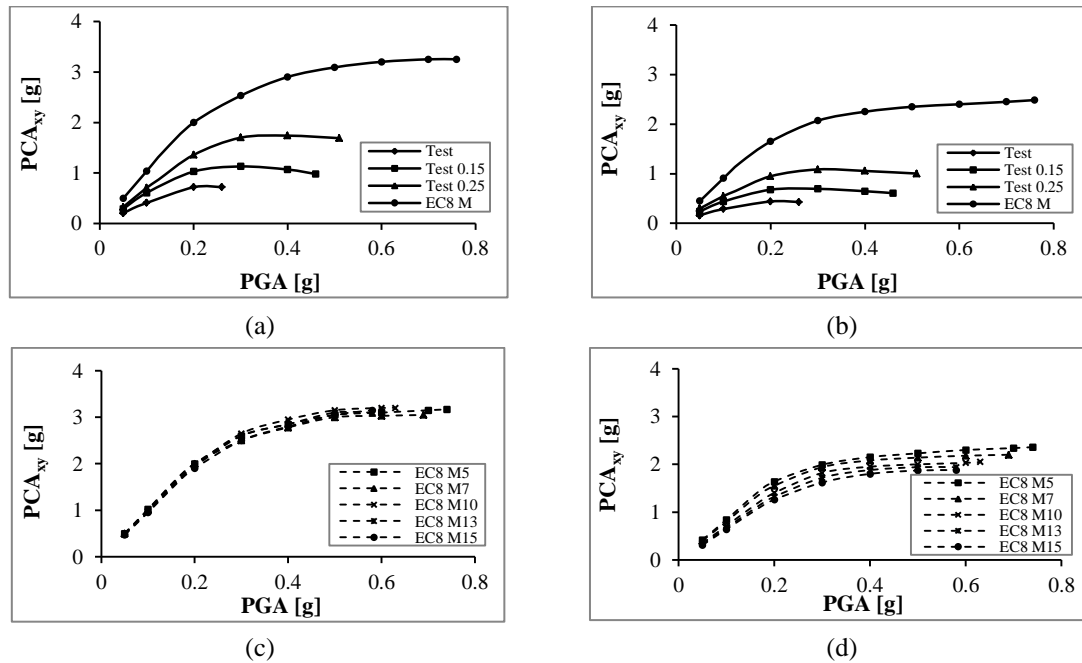

Fig. 8 Variation of peak component acceleration vs. peak ground acceleration for the NSCs with $T_C = T_1$ and attached to the top floors at: (a) flexible sides of the 1st group, (b) centres of rigidity of the 1st group, (c) flexible sides of the 2nd group, and (d) centres of rigidity of the 2nd group of buildings

Fig. 8(c) shows that the NSCs attached to the flexible sides of the second group of buildings had approximately the same acceleration response. However, Fig. 8(d) shows that the NSCs attached to the centres of rigidity of the second group of buildings had accelerations that were inversely proportional to the heights of the P-structures. Once more, this result suggests that the NSCs attached to the flexible sides of taller buildings were more affected by the torsional behaviour than those attached to the flexible sides of shorter buildings. This result will be further discussed in Section 7.4.

The component acceleration amplification factor, defined in this study as PCA_{xy}/PGA, accounts for the dynamic amplification in the acceleration response of NSCs. Fig. 9 shows that, for the NSCs considered in this study, the maximum values of the component acceleration amplification factor occurred at the PGA values corresponding to the elastic seismic capacities of the P-structures which are indicated by the vertical lines in Fig. 9. As explained above, within the elastic range of the P-structures, the acceleration values experienced by the NSCs increase with the increase in PGA. However, when the PGA value is further increased the P-structures experience damage and start to behave in-elastically which leads to changes in their dynamic characteristics i.e. increase in their vibration periods due to reduced stiffness. This reduces the resonance effect experienced by the NSCs. Hence, the maximum values of the component acceleration amplification factor occur at the elastic seismic capacities of the P-structures.
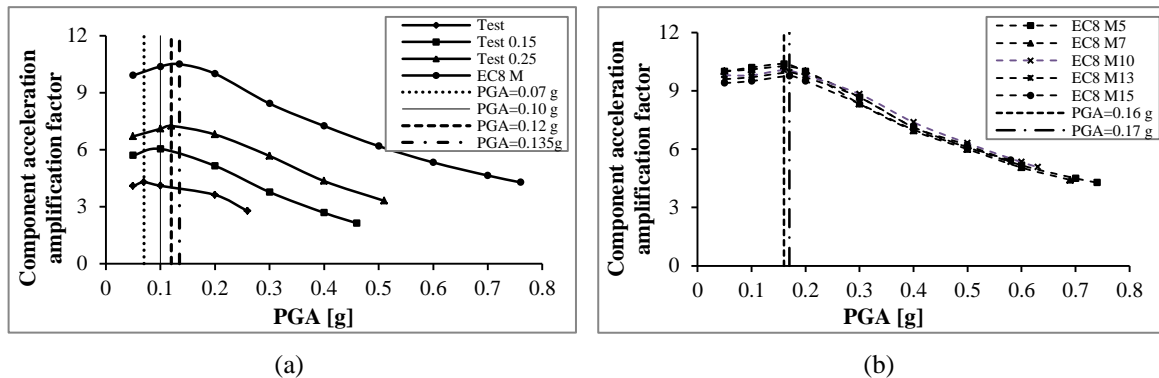

Fig. 9 Variation of component acceleration amplification factor vs. peak ground acceleration for the NSCs with $T_C = T_1$ and attached to the top floors of: (a) the 1st group of buildings and (b) the 2nd group of buildings

7.3 Effect of NSC to P-structure height ratio

Fig. 10 shows the relationship between NSC to P-structure height ratio (z/H) and peak component acceleration for the NSCs with $T_C = T_1$. The height ratio refers to the height (z) at which the NSC is located relative to the height of the building (H). The NSCs were attached at varying heights to the flexible sides (FS) and centres of rigidity (CR) of the P-structures designed according to EC8 (2004), i.e. EC8 M, EC8 M5, EC8 M7, EC8 M10, EC8 M 13, and EC8 M15. In each case, two PGA values corresponding to the elastic and maximum seismic capacities of each building were considered. The legend used in Fig. 10(a) applies to the remaining curves in Fig. 10.
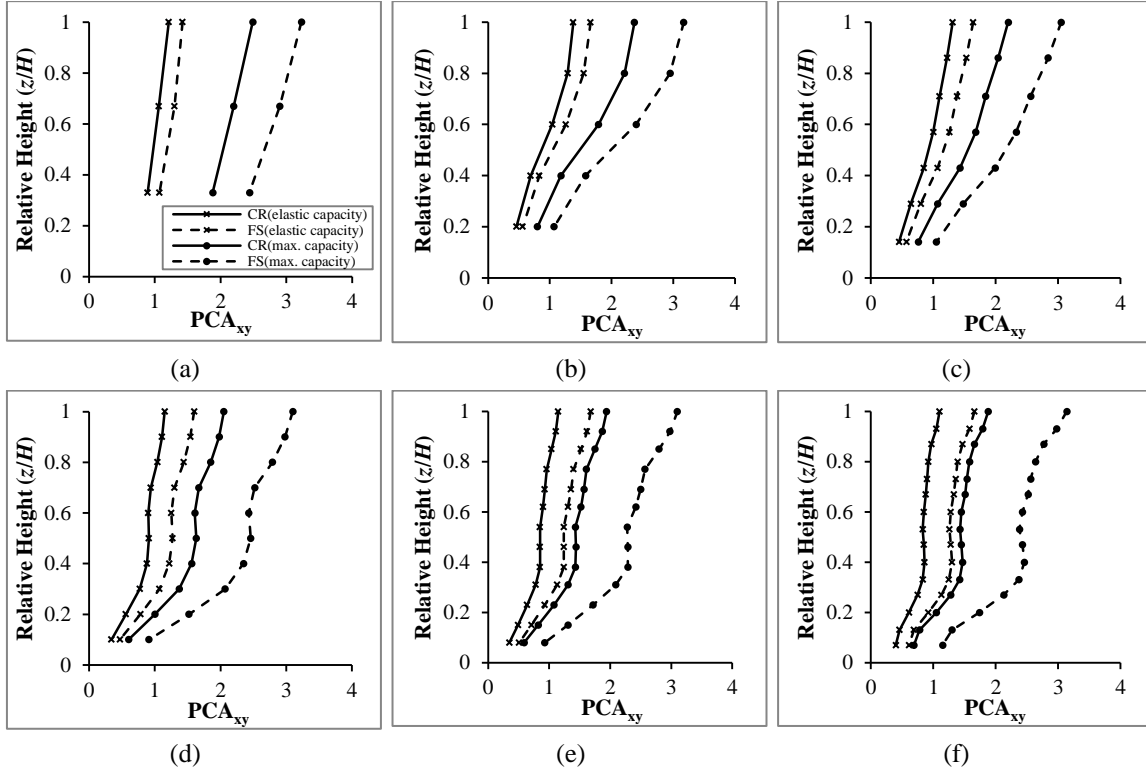
Fig. 10 Variation of NSC to P-structure height ratio vs. peak component acceleration for the NSCs with T_C = T_1 and attached to: (a) EC8 M, (b) EC8 M5, (c) EC8 M7, (d) EC8 M10, (e) EC8 M13 and (f) EC8 M15

The FE predictions suggest that the relationship between z/H and PCA_{xy} is linear in the case of EC8 M which had the least height (9 m) and fundamental vibration period (0.55 s). With the increase in the P-structures heights and fundamental vibration periods, the curves become piecewise-linear and then non-linear.

For a given building and a given PGA value, there are two curves showing the variations of z/H vs. PCA_{xy} for the NSCs attached to the FS and CR of the building. It can be noted that the acceleration values for the NSCs attached to the flexible sides were higher than the corresponding values for the NSCs attached to the centres of rigidity. Furthermore, the component acceleration values at the maximum seismic capacities were higher than the corresponding values at the elastic seismic capacities of the P-structures. These observations apply to all the NSCs considered in this study regardless of their z/H value or the P-structure height. For a given building, the NSCs attached to the top floor of the building, i.e., when z/H = 1.0, experienced the maximum accelerations regardless of the PGA value. This trend matches the EC8 (2004) design guidelines which will be detailed in Section 8.

7.4 Effect of P-strcurure torsional behaviour

The torsional amplification factor (F_T) for NSCs accelerations may be defined as the ratio of

peak component acceleration at the flexible side ($PCA_{xy,FS}$) to the corresponding value at the centre of rigidity ($PCA_{xy,CR}$) (Hart *et al.* 1975), i.e., ($F_T = PCA_{xy,FS}/PCA_{xy,CR}$). For the NSCs with $T_C = T_1$ and attached to the top floors of the *P*-structures considered in this study, Fig. 11 shows the variations of F_T and top floor rotation (θ) with *PGA*. The values of *PGA* considered were in the range of 0.05 g to the maximum seismic capacity of each building.

For the first group of buildings, Fig. 11(a) shows that Test experienced the highest top floor rotation of 0.0173 rad. and consequently had the most significant torsional behaviour. The torsional amplification factor for the NSCs attached to the flexible side of the top floor of Test was 1.75. The NSCs attached to the flexible sides of the top floors of Test 0.15 and Test 0.25 had F_T values of 1.67 and 1.70 respectively. These approximately equal F_T values may be explained by the fact that Test 0.15 and Test 0.25 had comparable top floor rotations (0.0155 rad. and 0.0162 rad. respectively) and consequently similar torsional behaviour. EC8 M had the least top floor rotation of 0.0069 rad. and the NSCs attached to the flexible side of this building had the least torsional amplification factor of 1.30.

For the second group of buildings, Fig. 11(b) shows that, at a given *PGA*, the torsional amplification factors and top floor rotations increased with the increase in total height of the P-structure. This result further clarifies why the NSCs with $T_C = T_1$ and attached to the top floors of EC8 M5, EC8 M10, and EC8 M15 had comparable acceleration values at the maximum seismic capacity of each building in spite of the different seismic capacities of the buildings (see Fig. 7(b)). The maximum seismic capacities of EC8 M5, EC8 M10, and EC8 M15 were 0.76 g, 0.63 g, and 0.58 g respectively. The NSCs with $T_C = T_1$ and attached to the top floors of these buildings had F_T values of 1.34, 1.56, and 1.65 respectively. It can be seen that EC8 M10 and EC8 M15 had higher torsional amplification factors than EC8 M5. This, in turn, resulted in the comparable NSCs accelerations at the different maximum seismic capacities of these buildings (see Fig. 7(b)).
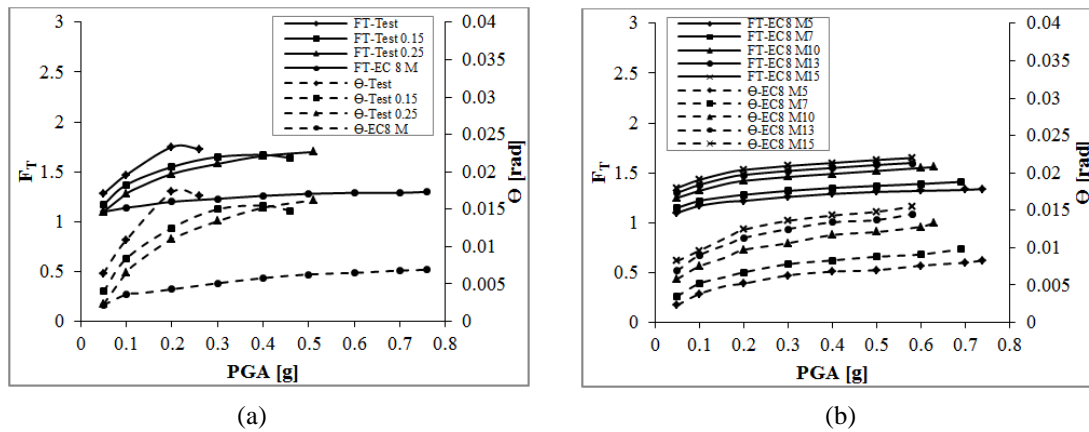

Fig. 11 Variations of top floor rotations and torsional amplification factor for the NSCs with $T_C = T_1$ vs. peak ground acceleration for: (a) the first group of buildings and (b) the second group of buildings

For a given P-structure, Fig. 11 suggests that there is a strong correlation between F_T and θ. Fig. 12 shows that the relationship between F_T and θ may be expressed as follows
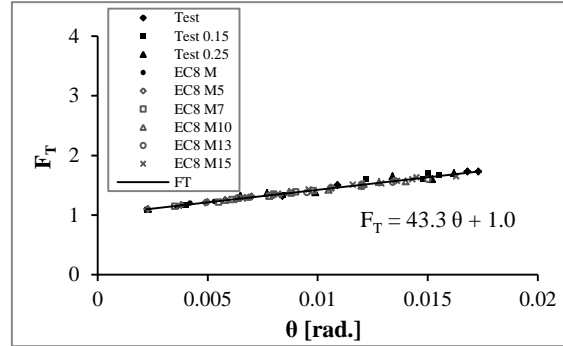
Fig. 12 Relationship between torsional amplification factor (F_T) and top floor rotation (θ)

$$F_T = 43.3\theta + 1.0 \tag{1}$$

Eq. (1) is valid for both regular and irregular P-structures. For a regular P-structure that does not experience floor rotations during earthquakes, Eq. (1) predicts a torsional amplification factor of 1.0. F_T becomes greater than 1.0 when the P-structure exhibits torsional behaviour. It can be concluded that the increase in θ, which is a measure of the torsional behaviour of the P-structure, results in a corresponding increase in F_T and consequently the accelerations of the NSCs attached to the flexible side of the P-structure. It is important to note that EC8 (2004) does not explicitly consider the increase in NSCs accelerations caused by the torsional behaviour of the P-structure.

8. Comparison between the FE results and EC8 recommendations

EC8 (2004) suggests the following expression for calculating the seismic coefficient applicable to non-structural elements (S_a)

$$S_a = \alpha S \left[\frac{3[1 + (z/H)]}{1 + [1 - (T_C/T_1)]^2} - 0.5 \right] \tag{2}$$

where
α is the ratio of the design ground acceleration on type A ground, a_g, to the acceleration of gravity;
S is the soil factor (based on EC8 (2004) Table 3.2, S is taken as 1.15 for ground type C and EC8 type 1 elastic response spectrum which is considered in this study);
T_C is the fundamental vibration period of the NSC;
T_1 is the fundamental vibration period of the building in the relevant direction;
z is the height of the NSC above the level of application of the seismic action; and
H is the building height measured from the level of application of the seismic action.
Hence, multiplying S_a, as given by Eq. (2), by the acceleration of gravity (g) yields the EC8 (2004) prediction for the design acceleration of NSCs. This approach was used to predict the accelerations of the NSCs with $T_C = T_1$ and attached at varying heights to the *P*-structures that

were in full conformity with EC8 (2004) provisions; i.e. EC8 M, EC8 M5, EC8 M7, EC8 M10, EC8 M13, and EC8 M15. These P-structures were designed for an a_g value of 0.25 g. Considering the soil factor of 1.15 for ground type C, the design PGA value was 0.29 g. Hence, the term αS in Eq. (1) was taken as 0.29.

As shown in Fig. 13, EC8 (2004) predicts a linear relationship between NSC to P-structure height ratio (z/H) and peak component acceleration (PCA_{xy}). For the NSCs attached to the ground levels of the P-structures ($z/H = 0$), EC8 (2004) predicts an acceleration of 0.725 g. For the NSCs attached to the top floors of the P-structures ($z/H = 1.0$), EC8 (2004) predicts an acceleration of 1.595 g. These predictions apply to all the NSCs attached to the above six P-structures regardless of the torsional behaviour of the P-structures. The FE results clearly demonstrated that the NSCs accelerations increase with the increase in floor rotations due to torsion. Nonetheless, Eq. (2) does not consider the amplification in the dynamic response of NSCs induced by the torsional behaviour of P-structures.

The above-mentioned six P-structures together with the NSCs with $T_C = T_1$ and attached to the P-structures at varying heights were numerically analysed under the PGA value of 0.29 g, i.e. the design PGA of the buildings. Fig. 13 compares the peak component accelerations obtained from the FE analyses with the corresponding values predicted by Eq. (2). Except for the case of EC8 M, EC8 (2004) reasonably predicted the component accelerations at the centres of rigidity with a mean predicted-to-numerical ratio of 0.94 and a standard deviation of 0.18. On the other hand, the EC8 (2004) predictions for the component accelerations at the flexible sides were alarmingly
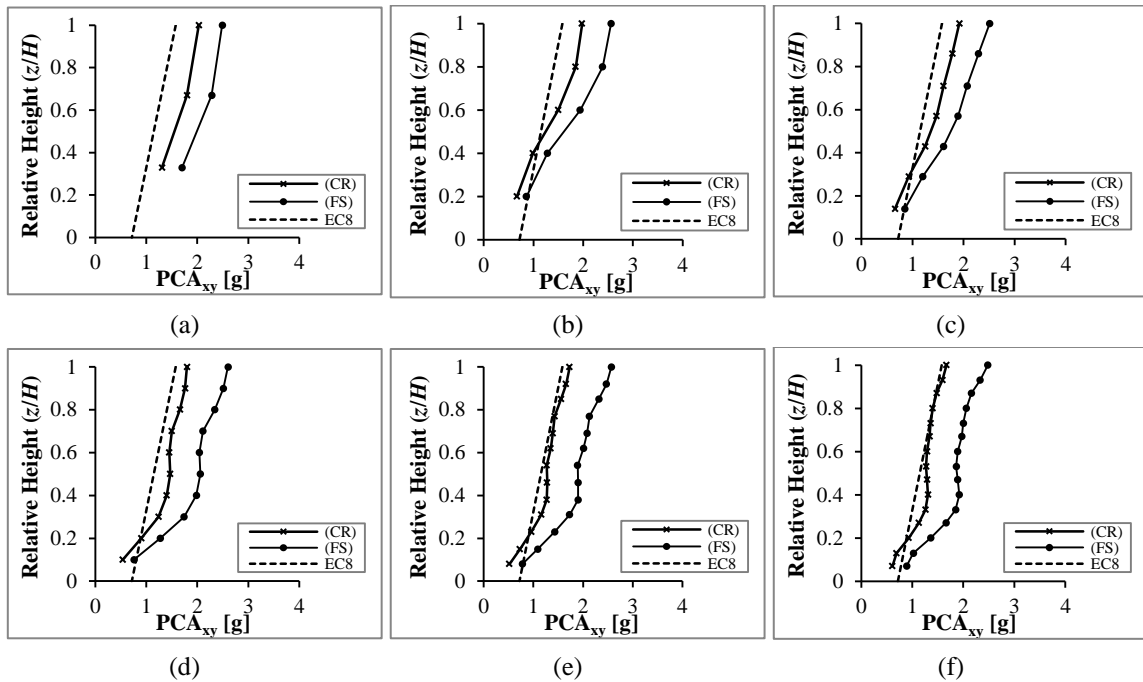

Fig. 13 Comparison between FE and EC8 acceleration predictions for the NSCs with $T_C = T_1$ and attached to the flexible side (FS) and centre of rigidity (CR) at the design peak ground acceleration of each building: (a) EC8 M, (b) EC8 M5, (c) EC8 M7, (d) EC8 M10, (e) EC8 M13, and (f) EC8 M15

underestimated with a mean predicted-to-numerical ratio of 0.67 and a standard deviation of 0.13. This result suggests that Eq. (2) needs to be modified so as to take into account the amplification in the dynamic response of NSCs caused by the torsional behaviour of *P*-structures.

9. Further considerations and future research

The research work presented in this paper focused on predicting the dynamic response of NSCs attached to irregular RC *P*-structures. The *P*-structures considered had a plan layout similar to physically tested and/or previously modelled buildings. This approach enabled the validation the FE code used in this study and established the credibility of the FE results. However, modern *P*-structures have different complicated plan layouts and/or mass irregularities along their heights. Such considerations should be the subject of further research aiming at confirming the accuracy of Eq. (1) and suggesting a modification for Eq. (2).

10. Conclusions

This study presents the results of a numerical investigation on the seismic response of NSCs mounted on irregular RC *P*-structures. The influence of NSC to *P*-structure vibration period ratio, peak ground acceleration, NSC to *P*-structure height ratio, and *P*-structure torsional behaviour on the seismic response of the NSCs was studied. The predictions of Eurocode 8 were compared with the numerical results. Based on the results of this study, the following conclusions are drawn:

1. As would be expected for near-resonance behaviour, a sharp increase in the dynamic response of the NSCs occurred when their vibration periods matched one of the vibration periods of the *P*-structures.
2. For $T_C = T_1$, the NSCs accelerations at the maximum seismic capacities were on average 125% and 91% higher than the corresponding values at the elastic seismic capacities of the first and second groups of buildings respectively.
3. For a given P-structure, the NSCs accelerations varied approximately linearly with base excitation up to the PGA value corresponding to the elastic seismic capacity of the P-structure. At higher PGA values, the relationship between NSCs accelerations and PGA was non-linear.
4. The NSCs attached to the flexible sides of the P-structures had accelerations that were on average 42% higher than the accelerations of the NSCs attached to the centres of rigidity.
5. The maximum values of the component amplification factor, defined as PCA_{xy}/PGA, occurred at the PGA values corresponding to the elastic seismic capacities of the P-structures.
6. The relationship between NSC to P-structure height ratio (z/H) and peak component acceleration was linear in the case of EC8 M which had the least height (9 m) and fundamental vibration period (0.55 s). With the increase in the P-structures heights and fundamental vibration periods, the curves become piecewise-linear and then non-linear. The maximum component accelerations predicted at the top floors, i.e. when $z/H = 1.0$.
7. The increase in the torsional behaviour of the P-structures resulted in a corresponding increase in the accelerations of the NSCs attached at the flexible sides of the studied P-structures.
8. Comparison between the FE results and EC8 recommendations suggests that, when the

fundamental periods and heights of the NSCs match those of the *P*-structures, EC8 underestimates the response of the NSCs mounted on the flexible sides of irregular RC P-structures with a mean predicted-to-numerical ratio of 0.67 and a standard deviation of 0.13. The perceived cause of this discrepancy is that EC8 does not take into account the amplification in the dynamic response of NSCs caused by the torsional behaviour of RC P-structures.

Acknowledgments

References

Agrawal, A. and Datta, T. (1997), "Behavior of secondary system attached to a torsionally coupled primary system", *Eur. Earthq. Eng.*, **11**, 47-53.

Agrawal, A. and Datta, T. (1998), "Seismic response of a secondary system mounted on a torsionally coupled non-linear primary system", *J. Earthq. Eng.*, **2**, 339-356.

Agrawal, A.K. (1999), "Non-linear response of light equipment system in a torsional building to bi-directional ground excitation", *Shock Vib.*, **6**, 223-236.

Aldeka, A., Chan, A. and Dirar, S. (2012), "Finite element modelling of non-structural components mounted on a torsionally multi-storey building", *Proceedings of the 20th UK Conference of the Association for Computational Mechanics in Engineering (ACME2012)*, Manchester, United Kingdom, March.

Aldeka, A., Chan, A. and Dirar, S. (2013a), "Finite element modelling of non-structural components mounted on irregular RC buildings", *Proceedings of the International Conference on Computational Mechanics (CM13)*, Durham, United Kingdom, March.

Aldeka, A., Chan, A. and Dirar, S. (2013b), "Effects of torsion on the behaviour of non-structural components mounted on irregular reinforced concrete multi-storey buildings", *Proceedings of the 4th ECCOMAS Thematic Conference on Computational Methods in Structural Dynamics and Earthquake Engineering*, Kos Island, Greece, June.

Chandler, A. and Hutchinson, G. (1986), "Torsional coupling effects in the earthquake response of asymmetric buildings", *Eng. Struct.*, **8**, 222-236.

Chaudhuri, S.R. and Villaverde, R. (2008), "Effect of building nonlinearity on seismic response of nonstructural components: a parametric study", *J. Struct. Eng. - ASCE*, **134**, 661-670.

Chen, Y. and Soong, T. (1988), "Seismic response of secondary systems", *Eng. Struct.*, **10**, 218-228.

EC8 (2004), EN 1998-1 Eurocode 8, Design of structures for earthquake resistance, Part 1: General rules, seismic actions and rules for buildings, European Committee for Standardization Brussels, Belgium.

ESD European Strong motion Database, http://www.isesd.cv.ic.ac.uk/.

Fajfar, P., Marušić, D. and Peruš, I. (2005), "Torsional effects in the pushover-based seismic analysis of buildings", *J. Earthq. Eng.*, **9**, 831-854.

Graves, H. and Morante, R. (2006), *Recommendations for revision of seismic damping values in Regulatory Guide 1.61*, U.S. Nuclear Regulatory Commission Office of Nuclear Regulatory Research Washington, DC 20555-000.

Hart, G.C., Lew, M. and DiJulio, R.M. (1975), "Torsional response of high-rise buildings", *J. Struct. Div.*,

101, 397-416.

Iervolino, I., Maddaloni, G. and Cosenza, E. (2009), "A note on selection of time-histories for seismic analysis of bridges in Eurocode 8", *J. Earthq. Eng.*, **13**, 1125-1152.

Iervolino, I., Galasso, C. and Cosenza, E. (2010), "REXEL: computer aided record selection for code-based seismic structural analysis", *Bull. Earthq. Eng.*, **8**, 339-362.

Kreslin, M. and Fajfar, P. (2010), "Seismic evaluation of an existing complex RC building", *Bull. Earthq. Eng.*, **8**, 363-385.

Mander, J., Priestley, M.N. and Park, R. (1988), "Theoretical stress-strain model for confined concrete", *J. Struct. Eng. - ASCE*, **114**, 1804-1826.

Menegotto, M. and Pinto, P.E. (1973), "Method of analysis for cyclically loaded RC plane frames including changes in geometry and non-elastic behaviour of elements under combined normal force and bending", *Symposium on the Resistance and Ultimate Deformability of Structures acted on by well defined loads*, International Association for Bridge and Structural Engineering, Zurich, Switzerland.

MIDAS Gen (2012), *Analysis manual*, version 3.1, http://www.MidasUser.com/.

Mohammed, H.H., Ghobarah, A. and Aziz, T.S. (2008), "Seismic response of secondary systems supported by torsionally yielding structures", *J. Earthq.Eng.*, **12**, 932-952.

Negro, P., Mola, E., Molina, F.J. and Magonette, G.E. (2004), "Full-scale PSD testing of a torsionally unbalanced three-storey non-seismic RC frame", *Proceedings of 13th WCEE, 2004. 13th World conference on Earthquake Engineering*, Vancouver, Canada, No. 968.

Oropeza, M., Favez, P. and Lestuzzi, P. (2010), "Seismic response of nonstructural components in case of nonlinear structures based on floor response spectra method", *Bull. Earthq. Eng.*, **8**, 387-400.

Paz, M. (1994), *International handbook of earthquake engineering codes, programs, and examples*, Springer.

Phan, L.T. and Taylor, A.W. (1996), "State of the art report on seismic design requirements for nonstructural building components", Report NISTIR 5857, National Institute of Standards and Technology, Gaithersburgh, MD.

Rozman, M. and Fajfar, P. (2009), "Seismic response of a RC frame building designed according to old and modern practices", *Bull. Earthq. Eng.*, **7**, 779-799.

Sackman, J.L. and Kelly, J.M. (1979), "Seismic analysis of internal equipment and components in structures", *Eng. Struct.*, **1**, 179-190.

Seismosoft (2009), SeismoMatch version 2.1, http://www.seismosoft.com/.

SIMQKE (1976), *User manual*, NISEE software library, University of California, Berkeley, USA.

Stefano, D.M. and Pintucchi, B. (2010), "Predicting torsion-induced lateral displacements for pushover analysis: influence of torsional system characteristics", *Earthq. Eng.Struct. Dyn.*, **39**, 1369-1394.

Villaverde, R. (1997), "Seismic design of secondary structures: state of the art", *J. Struct. Eng. - ASCE*, **123**, 1011-1019.

Whittaker, A. and Soong, T. (2003), "An overview of nonstructural components research at three US earthquake engineering research centers", *Proceedings of ATC-29-2 Seminar on Seismic Design, Performance, and Retrofit of Nonstructural Components in Critical Facilities*, ATC-29-2 Report, Applied Technology Council, Redwood City, California.

Yang, Y.B. and Huang, W.H. (1993), "Seismic response of light equipment in torsional buildings", *Earthq. Eng. Struct. Dyn.*, **22**, 113-128.

Yang, Y.B. and Huang, W.H. (1998), "Equipment–structure interaction considering the effect of torsion and base isolation", *Earthq. Eng. Struct. Dyn.*, **27**, 155-171.

IT